

GEOMETRIC RESTRUCTURIZATION OF THE SPACE OBJECT TRACKING PROBLEM FOR IMPROVED UNCERTAINTY REPRESENTATION

J. T. Kent⁽¹⁾, S. Bhattacharjee⁽¹⁾, I. Hussein⁽²⁾, and M. K. Jah⁽³⁾

⁽¹⁾University of Leeds, Leeds, LS2 9JT, UK, Email: {j.t.kent, mmsb}@leeds.ac.uk

⁽²⁾Applied Defense Solutions, Columbia, MD 21044, USA, Email: ihussein@applieddefense.com

⁽³⁾University of Texas at Austin, Austin, TX 78712, USA, Email: moriba@utexas.edu

ABSTRACT

The problem of space debris tracking can be viewed as an example of Bayesian filtering. Examples of such filters include the classic Kalman filter, together with nonlinear variants such as the extended and unscented Kalman filters, and the computationally more expensive particle filters. The purpose of this paper is to show with a careful choice of coordinate system, the uncertainty in the space debris tracking problem can often be formulated in terms of a multivariate normal distribution, and hence filtering can be carried out using the Kalman Filter or one of its variants.

Keywords: Bayesian filtering, Uncertainty propagation.

1. INTRODUCTION

An object orbiting the earth follows an elliptical path, ignoring perturbation effects. The simplest way to describe the orbit is to specify the position and velocity of the object, a six-dimensional quantity, in earth-centered inertial (ECI) coordinates. However, even if the initial uncertainty of the object is normally distributed, the propagated uncertainty of the object after orbiting for several periods becomes distinctly non-normal. In particular, the shape of the point cloud for position becomes increasingly “banana-shaped” [2].

In general, the filtering problem is simplest when the joint distribution of the state vector and the observation vector is normally distributed. However, as just noted, ECI coordinates are not very suitable other than for short term propagation. It is tempting to consider one of the other coordinate systems used for orbiting objects, such as Keplerian orbital elements and equinoctial orbital elements. Unfortunately, these coordinate systems do not generally preserve normality either.

Hence, in this paper we introduce a new coordinate system called “adaptive structural coordinates” to describe the orbiting object. The key idea is to use certain tangent

coordinates to describe the uncertainties in the parameters of interest. The phrase “adaptive” means that if the center of the distribution changes as new data arrive, then the choice of tangent projection changes. The key ingredients of this 6-dimensional coordinate system are as follows:

- An ellipse in the plane can be described in terms of a symmetric positive definite 2×2 matrix. The eigenvectors represent the directions of the major and minor axes and the ratio of eigenvalues determines the ellipticity. Uncertainties in the three distinct entries of this matrix will typically be approximately normally distributed.
- The normal direction to the elliptical plane can be viewed as a point on the unit sphere. Uncertainty in this direction can be represented in tangent coordinates to the sphere, a two-dimensional quantity.
- One coordinate is needed to describe the displacement of the object along the ellipse. We shall use the mean anomaly. Typically, the mean anomaly is treated as an angle on the circle, but if we keep track of the winding number during the propagation step, the “unwound” version can be treated as a real number. This coordinate propagates nonlinearly, but uncertainty tends to remain normal.

For an orbiting object following Keplerian dynamics, the first five adaptive structural coordinates remain unchanged in time; only the mean anomaly changes over time.

The paper is organized as follows. First we discuss why Keplerian and equinoctial coordinates can sometimes fail to preserve normality under propagation. In particular, we consider a simple example based on spherical coordinates and describe situations under which they will or will not tend to have normal distributions.

Next we look at the behavior of the propagated uncertainty under the four coordinate systems described.

Finally, we discuss briefly how these propagation calculations can be combined with angles-only observational data to carry out an update step for the Bayesian filter.

2. SINGULARITIES AND DISTORTIONS IN COORDINATE SYSTEMS

Coordinate systems can be classified into two categories: global and local. ECI, Keplerian and equinoctial elements are examples of global coordinate systems, whereas adaptive structural coordinates are local. Global coordinates can fail to preserve normality for two main reasons:

- *Curvature.* This problem is best illustrated in ECI coordinates, where the uncertainty spreads out along a curved path. Switching to spherical coordinates can fix this problem for the position vector (see, e.g. [3]-[4]), but a more comprehensive solution is given by the adaptive structural coordinates used here.
- *Bounded range.* For some of the parameters, there may be a natural finite range. For example, ellipticity of an ellipse lies between 0 and 1. Similarly, the latitude of a point on the sphere ranges between -90° and 90° . Further, these endpoints are often achievable: an ellipse with zero ellipticity is a circle, and latitude 90° corresponds to the north pole. If uncertainty is concentrated near one of these endpoints, then the resulting distribution cannot be normal; the best it can be is folded normal, but often the behavior is even more complicated to describe.

A simple example to illustrate the problems with bounded range is given by the unit sphere, where points can be represented either in cartesian coordinates (y_1, y_2, y_3) or in spherical coordinates, θ and ϕ ,

$$y_1 = \cos \theta \cos \phi, \quad y_2 = \cos \theta \sin \phi, \quad y_3 = \sin \theta.$$

Here $\theta \in [-90^\circ, 90^\circ]$ denotes the latitude and $\phi \in [-180^\circ, 180^\circ]$ is the longitude.

Consider a highly concentrated distribution on the sphere (more specifically, a Fisher distribution with concentration parameter $\kappa = 2500$), with two possible centers.

- The first center lies on the equator at $(1, 0, 0)$ with $\theta_0 = 0^\circ$, $\phi_0 = 0^\circ$.
- The second center lies at the north pole $(0, 0, 1)$ with $\theta_0 = 90^\circ$ and ϕ_0 undefined.

Point clouds for simulated values of ϕ and $\sin \theta$ are plotted in Fig. 1. For the first distribution (A), θ lies a long way from its endpoints, and the distributions of ϕ and

$\sin \theta \approx \theta$ look normal (top line of Fig. 2). For the second distribution (B), $\theta_0 = 90^\circ$ lies at the endpoint of possible values. In this case the distribution of $1 - \sin \theta$ approximately follows an exponential distribution and ϕ is uniformly distributed on the circle (bottom line of Fig. 2), both of which are very non-normal.

For parameters lying on a sphere, our strategy is to orient the coordinate system to be like the first case rather than the second case. A similar, but technically more involved, strategy is used to represent a set of nearby planes in a common planar coordinate system.

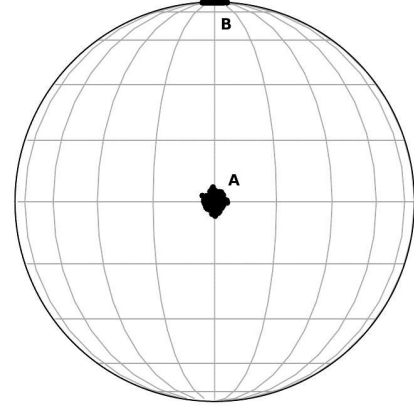


Figure 1. The unit sphere with two concentrated point clouds plotted, one near the equator (A) and one near the north pole (B).

PROPAGATING UNCERTAINTY

For the space object tracking problem, a simulation has been carried out to assess the normality of the 6 coordinates for three global coordinate systems and for our new adapted structural coordinates. A short summary of each global coordinate system is given below :

- **ECI** An object is represented by a three-dimensional position vector and a three-dimensional velocity vector.
- **Keplerian orbital elements** are represented using semi-major axis (a), eccentricity (e), inclination (i), RAAN (Ω), argument of perigee (ω) and mean anomaly (M_0). The eccentricity is bounded by 0 and 1, and the inclination lies on the bounded interval, $[0^\circ, 180^\circ]$. The other angular components Ω , ω , M_0 , lie on the circle. For the mean anomaly, it also makes sense to treat it as a real number by counting its winding number from the initial to the current time. For this study the unwrapped version of the mean anomaly is used.
- **Equinoctial orbital elements** are represented using a , $h = e \sin(\Omega + \omega)$, $k = e \cos(\Omega + \omega)$, $p = \tan(i/2) \sin(\Omega)$, $q = \tan(i/2) \cos(\Omega)$ and $\lambda = \Omega +$

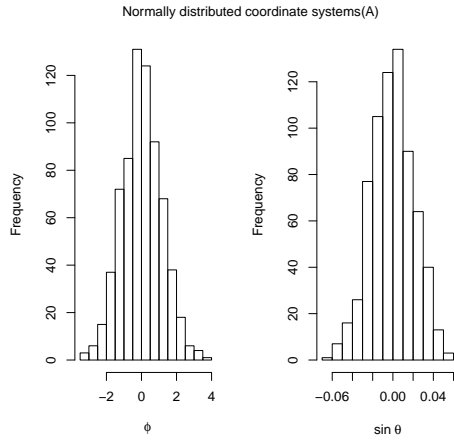


Figure 2. Spherical coordinates for two distributions on the sphere: A. top line; B. bottom line.

$\omega + M_0$. When the inclination angle i approaches 180° , p and q become ill-defined. The last element is the sum of three angular elements.

Example 1. To illustrate the ideas in this paper consider a space object in an elliptical orbit with eccentricity $e = 0.72$. The orbital period is $p = 724$ minutes here and the inclination is 180° . Starting from small isotropic normal uncertainties in the position and velocity in ECI coordinates at initial time $t = 0$, the object has been propagated for 4.26 times its orbital period. A *pairs plot* giving marginal histograms and bivariate scatter plots has been produced for each of the four coordinate systems (Figs. 3–6).

To some extent this example has been tuned to show Keplerian and equinoctial elements in a bad light. On the other hand the normal-looking shape of the point clouds for the adaptive structural coordinates seems fairly universal, even under the extreme value for the ellipticity parameter used here, $e = 0.72$.

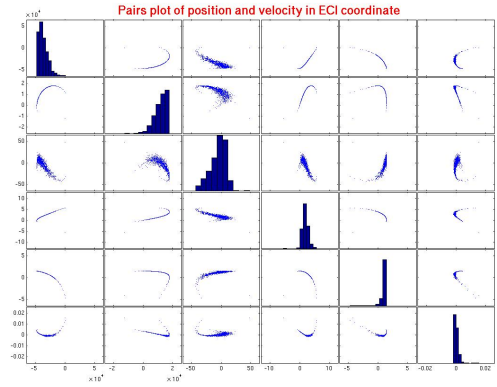


Figure 3. Example 1. Six-dimensional pairs plot for position (three-dimensional) and velocity (three-dimensional) for ECI coordinates.

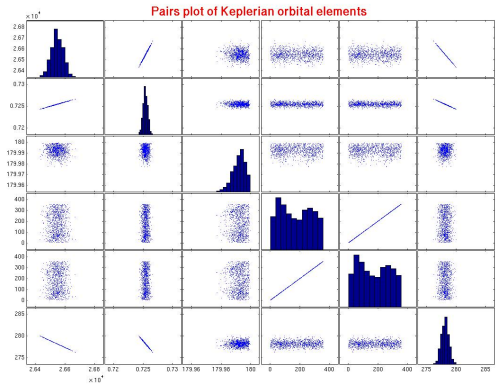
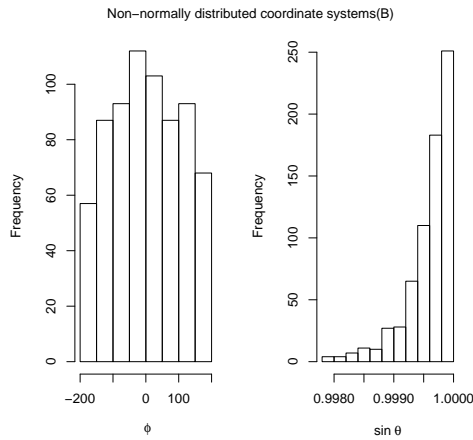


Figure 4. Example 1. Six-dimensional pairs plot for Keplerian orbital elements.

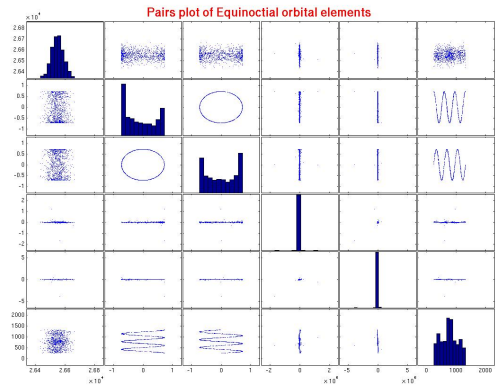


Figure 5. Example 1. Six-dimensional pairs plot for equinoctial orbital elements.

A number of features are immediately apparent in these plots.

- ECI coordinates (Fig. 3). Strong curvature is ap-

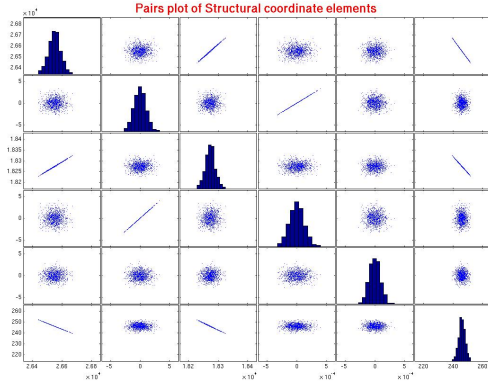


Figure 6. Example 1. Six-dimensional pairs plot for the adaptive structural coordinates.

parent in all the pairs plots. These plots are very non-normal.

- *Keplerian orbital elements* (Fig. 4). Some of the plots are very non-normal. In particular variables 4 and 5 are approximately uniformly distributed on the circle.
- *Equinoctial orbital elements* (Fig. 5). Some of the plots are very non-normal, especially the high concentration on the circumference of an ellipse for the scatter plot of variable 2 vs. variable 3.
- *Adapted structural coordinates* (Fig. 6). All the histograms and all the scatter plots look approximately normal. Note that in plots such as variable 1 vs. variable 3, the apparent line segment is really a highly eccentric ellipse.

Example 2. In this example an object with medium eccentricity ($e = 0.14$) is considered with inclination 0° . The orbital period is $p = 132$ minutes and the object is propagated for 4.26 orbital periods.

Just as in the previous example, it can be seen that the coordinates for the adaptive structural coordinates system (Fig. 10) are approximately normally distributed. For other coordinate systems there are generally some problems. The ECI coordinate system (Fig. 7) shows the same sort of curvature as before. For Keplerian orbital elements (Fig. 8), variables 4 and 5 are again approximately uniform on the circle.

The distributions of the equinoctial orbital elements (Fig. 9) are much closer to normality than in Example 1. However, note that the histograms for the second and third equinoctial orbital elements contain some outliers. The two modes for variable 6 are a minor artefact due to treating λ as a number rather than an angle (see [1] for further discussion).

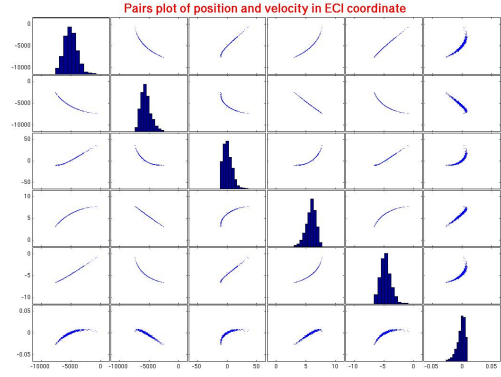


Figure 7. Example 2. Six-dimensional pairs plot for position (three-dimensional) and velocity (three-dimensional) for ECI coordinates.

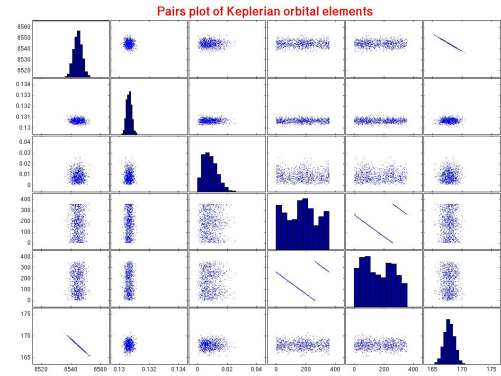


Figure 8. Example 2. Six-dimensional pairs plot for Keplerian orbital elements.

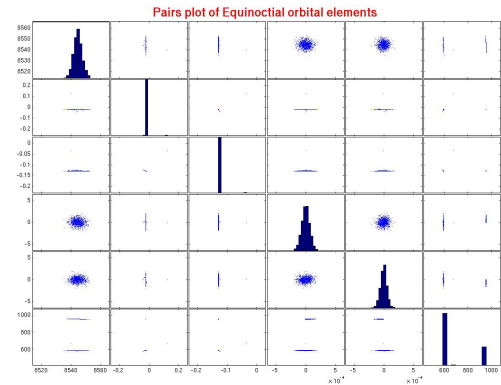


Figure 9. Example 2. Six-dimensional pairs plot for equinoctial orbital elements.

FUTURE WORK

So far we have concentrated on the propagation step in filtering. It remains to carry out the update step of the

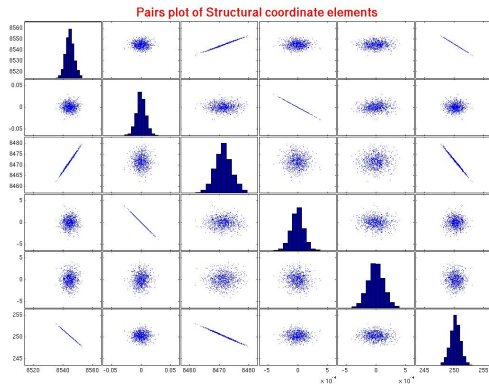


Figure 10. Example 2. Six-dimensional pairs plot for the adaptive structural coordinates.

filter by incorporating observational data.

A typical observation might consist of an angles-only measurement of the direction of the space object from a ground-based observer, assumed to follow a Fisher distribution with high concentration. With a suitable tangent projection, the tangent coordinates of these observations will be approximately normal.

Hence the joint distribution of the propagated state vector in adapted structural coordinates and the angles-only observation in spherical tangent coordinates is approximately 8-dimensional normal. Hence the update step for the Kalman filter or one of its variants seems appropriate here. Based on preliminary results and initial analyses, this approach seems very effective. Work is in progress to assess more fully its strengths and limitations.

ACKNOWLEDGMENTS

This material is based upon work supported by the Air Force Office of Scientific Research, Air Force Material Command, USAF under Award No. FA9550-16-1-0099.

REFERENCES

1. Horwood, J.T. and Poore, A. B. (2014). Gauss von Mises distribution for improved uncertainty realism in space situational awareness. *SIAM/ASA J. Uncertainty Quantification*, **2**, 276–304
2. Junkins, J.L., Akella, M. and Alfriend, K. (1996). Non-Gaussian error propagation in orbital mechanics. *Journal of the Astronautical Sciences*, **44**, 541–563
3. Kent, J.T., Hussein, I. and Jah, M.K. (2016). Directional distributions in tracking of space debris. *Proceedings of the 19th International Conference on Information Fusion (FUSION)*, Heidelberg, Germany, IEEE, 2081–2086

4. Kent, J.T., Bhattacharjee, S., Hussein, I. and Jah, M.K. (2017). Orbital error propagation analysis using directional statistics for space objects. *Proceedings of the 27th AAS/AIAA Space Flight Mechanics Meeting, San Antonio, Texas, February 5-9, 2017*, 1245–1254